J|A|C|S
ARTICLES
Published on Web 02/04/2004

Equilibrium Thermodynamic Studies in Water: Reactions of Dihydrogen with Rhodium(III) Porphyrins Relevant to Rh−Rh, Rh−H, and Rh−OH Bond Energetics

Xuefeng Fu and Bradford B. Wayland*

Contribution from the Department of Chemistry, University of Pennsylvania, Philadelphia, Pennsylvania 19104-6323

Received October 24, 2003; E-mail: wayland@sas.upenn.edu

Abstract: Aqueous solutions of rhodium(III) tetra *p*-sulfonatophenyl porphyrin ((TSPP)Rh(III)) complexes react with dihydrogen to produce equilibrium distributions between six rhodium species including rhodium hydride, rhodium(I), and rhodium(II) dimer complexes. Equilibrium thermodynamic studies (298 K) for this system establish the quantitative relationships that define the distribution of species in aqueous solution as a function of the dihydrogen and hydrogen ion concentrations through direct measurement of five equilibrium constants along with dissociation energies of D_2O and dihydrogen in water. The hydride complex ($[(TSPP)Rh-D(D_2O)]^{-4}$) is a weak acid ($K_a(298\ K) = (8.0 \pm 0.5) \times 10^{-8}$). Equilibrium constants and free energy changes for a series of reactions that could not be directly determined including homolysis reactions of the $Rh^{II}-Rh^{II}$ dimer with water (D_2O) and dihydrogen (D_2) are derived from the directly measured equilibria. The rhodium hydride $(Rh-D)_{aq}$ and rhodium hydroxide $(Rh-OD)_{aq}$ bond dissociation free energies for $[(TSPP)Rh-D(D_2O)]^{-4}$ and $[(TSPP)Rh-OD(D_2O)]^{-4}$ in water are nearly equal ($Rh-D = 60 \pm 3$ kcal mol^{-1}, $Rh-OD = 62 \pm 3$ kcal mol^{-1}). Free energy changes in aqueous media are reported for reactions that substitute hydroxide (OD^-) (-11.9 ± 0.1 kcal mol^{-1}), hydride (D^-) (-54.9 kcal mol^{-1}), and $(TSPP)Rh^{I}$: (-7.3 ± 0.1 kcal mol^{-1}) for a water in $[(TSPP)Rh^{III}(D_2O)_2]^{-3}$ and for the rhodium hydride $[(TSPP)Rh-D(D_2O)]^{-4}$ to dissociate to produce a proton (9.7 ± 0.1 kcal mol^{-1}), a hydrogen atom ($\sim 60 \pm 3$ kcal mol^{-1}), and a hydride (D^-) (54.9 kcal mol^{-1}) in water.

Introduction

Rhodium porphyrins accomplish a remarkable array of organometallic substrate reactions in both organic[1−5] and aqueous media.[6] Reactions of substrates such as H_2, CH_4, CO, and aldehydes with rhodium porphyrins that achieve observable equilibria in benzene provide one of the more reliable and extensive sets of organo-transition metal bond dissociation enthalpies (BDE) in organic media.[7,8] Current interest in converting organometallic processes from organic to aqueous media[9−11] has stimulated us to direct our attention toward evaluating the scope of organometallic reactions and thermodynamic parameters for rhodium porphyrin species in water.[6] Interpretation of thermodynamic measurements in water is complicated by solvation energies,[12,13] but aqueous media have the advantageous property that the equilibrium distribution of species can often be tuned by changing the hydrogen ion concentration which provides a strategy for evaluating equilibrium constants that are either too large or too small for direct measurement. This Article describes a set of simultaneous equilibria that result from reactions of dihydrogen (H_2/D_2) with rhodium(III) porphyrin aquo and hydroxo complexes in water that form rhodium hydride, rhodium(I), and rhodium(II) com-

(1) (a) Cui, W.; Zhang, X. P.; Wayland, B. B. *J. Am. Chem. Soc.* **2003**, *125*, 4994. (b) Zhang, X.-X.; Wayland, B. B. *J. Am. Chem. Soc.* **1994**, *116*, 7897. (c) Zhang, X.-X.; Park, G. F.; Wayland, B. B. *J. Am. Chem. Soc.* **1997**, *119*, 7938. (d)Wayland, B. B.; Sherry, A. E.; Bunn, A. G. *J. Am. Chem. Soc.* **1993**, *115*, 7675. (e) Bunn, A. G.; Wayland, B. B. *J. Am. Chem. Soc.* **1992**, *114*, 6917. (f) Sherry, A. E.; Wayland, B. B. *J. Am. Chem. Soc.* **1990**, *112*, 1259.
(2) (a) Aoyama, Y.; Fujisawa, T.; Toi, H.; Ogoshi, H. *J. Am. Chem. Soc.* **1986**, *108*, 943. (b) Aoyama, Y.; Yamagishi, A.; Tanaka, Y.; Toi, H.; Ogoshi, H. *J. Am. Chem. Soc.* **1987**, *109*, 4735.
(3) (a) Collman, J. P.; Boulatov, R. *Inorg. Chem.* **2001**, *40*, 2461. (b) Collman, J. P.; Boulatov, R. *Inorg. Chem.* **2001**, *40*, 560. (c) Collman, J. P.; Boulatov, R. *J. Am. Chem. Soc.* **2000**, *122*, 11812.
(4) (a) Nelson, A. P.; DiMagno, S. G. *J. Am. Chem. Soc.* **2000**, *122*, 8569. (b) Sun, H.; Xue, F.; Nelson, A. P.; Redepenning, J.; DiMagno, S. G. *Inorg. Chem.* **2003**, *42*, 4507.
(5) (a) Mak, K. W.; Chan, K. S. *J. Am. Chem. Soc.* **1998**, *120*, 9686. (b) Mak, K. W.; Yeung, S. K.; Chan, K. S. *Organometallics* **2002**, *21*, 2362.
(6) Fu, X.; Basickes, L.; Wayland, B. B. *Chem. Commun.* **2003**, 520.
(7) Wayland, B. B. *Polyhedron* **1988**, *7*, 1545.
(8) Wayland, B. B. In *Energetics of Organometallic Species*; Simões, J. A. M., Ed.; NATO Advanced Study Institute C; Kluwer Academic Publishers: Dordrecht, The Netherlands, 1992; Vol. 367, pp 69−74.
(9) (a) Cornils, B.; Kuntz, E. G. In *Aqueous-phase Organometallic Catalysis, Concept and Application*; Cornils, B., Herrmann, A. W., Eds.; Wiley-VCH: New York, 1998; Chapter 6. (b) Lucey, D. W.; Helfer, D. S.; Atwood, J. D. *Organometallics* **2003**, *22*, 826. (c) Lucey, D. W.; Atwood, J. D. *Organometallics* **2002**, *21*, 2481.
(10) (a) Stahl, S. S.; Labinger, J. A.; Bercaw, J. E. *Angew. Chem., Int. Ed.* **1998**, *37*, 2181. (b) Stahl, S. S.; Labinger, J. A.; Bercaw, J. E. *J. Am. Chem. Soc.* **1996**, *118*, 5961. (c) Lynn, D. M.; Grubbs, R. H. *J. Am. Chem. Soc.* **2001**, *123*, 3187. (d) Lynn, D. M.; Mohr, B.; Grubbs, R. H.; Henling, L. M.; Day, M. W. *J. Am. Chem. Soc.* **2000**, *122*, 6601.
(11) (a) Joo, F. *Acc. Chem. Res.* **2002**, *35*, 738. (b) Kovacs, J.; Todd, T. D.; Reibenspies, J. H.; Joo, F.; Darensbourg, D. J. *Organometallics* **2000**, *19*, 3963. (c) Joo, F.; Kovacs, J.; Benyei, A. C.; Nadasdi, L.; Laurenczy, G. *Chem.-Eur. J.* **2001**, *7*, 193.
(12) (a) Cramer, C. J.; Truhlar, D. G. *Chem. Rev.* **1999**, *99*, 2161. (b) Abraham, M. H.; Whiting, G. S.; Fuchs, R.; Chambers, E. J. *J. Chem. Soc., Perkin Trans.* **1990**, *2*, 291.
(13) (a) Ben-Naim, A. *J. Chem. Phys.* **1989**, *90*, 7412. (b) Ben-Naim, A.; Mazo, R. *J. Phys. Chem. B* **1997**, *101*, 11221. (c) Kanabus-Kaminska, J. M.; Gilbert, B. C.; Griller, D. *J. Am. Chem. Soc.* **1989**, *111*, 3311.

Table 1. Characteristic ^{1}H NMR Shifts (ppm) for (TSPP)Rh Species at 298 K in D_2O[a]

(TSPP)Rh	(TSPP)Rh complexes	pyrrole	phenyl	
			o-phenyl	m-phenyl
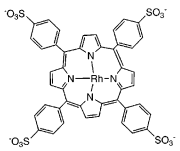	$[(TSPP)Rh^{III}(D_2O)_2]^{-3}$ (**2**)	9.15	8.44	8.25
	$[(TSPP)Rh^{III}(D_2O)(OD)]^{-4}$ (**3**)	9.04	8.43	8.25
	$[(TSPP)Rh^{III}(OD)_2]^{-5}$ (**4**)	8.94	8.44	8.24
	$[(TSPP)Rh\text{-}D(D_2O)]^{-4}$ (**5**)*	8.78	8.27	8.20
	$[(TSPP)Rh^{I}(D_2O)]^{-5}$ (**6**)	8.32	8.20	8.11
	$[(TSPP)Rh^{II}(D_2O)]_2^{-8}$ (**7**)	8.46	9.51, 6.95	8.47, 7.80

[a] The $[(TSPP)Rh-D(D_2O)]^{-4}$ (**5**) phenyl ^{1}H NMR spectrum is an AB pattern (8.27 ppm, 8.20 ppm) at 360 K, but it is a single exchange broadened peak centered at 8.25 ppm at 298 K in D_2O.

plexes. Each of these types of rhodium porphyrin species (Rh(I), Rh(II), Rh(III), Rh−H, and Rh−OH) functions as a precursor for a group of organometallic substrate reactions.[6,14] The detailed equilibrium studies presented in this Article establish a foundation for equilibrium thermodynamic studies in aqueous media for substrate reactions associated with these organometallic precursor species and also report on the direct evaluation of the acid dissociation constant for the Rh−H along with estimates of the rhodium−hydride and rhodium−hydroxide bond dissociation free energies in water.

Results

Aqueous solutions of rhodium(III) tetra *p*-sulfonatophenyl porphyrin ((TSPP)Rh(III)) complexes react with dihydrogen to produce equilibrium distributions between six rhodium species including rhodium hydride, rhodium(I), rhodium(II) dimer, and three rhodium(III) aquo and hydroxo complexes. Each of these (TSPP)Rh species can be readily distinguished by ^{1}H NMR spectroscopy in D_2O (Table 1). The porphyrin pyrrole and phenyl ^{1}H NMR shifts that are used in identifying the (TSPP)Rh species in D_2O are listed in Table 1. In aqueous solution, water molecules are assigned to axial rhodium coordination sites so as to produce an electronically saturated (18-electron) metal center. ^{1}H NMR shift and intensity measurements were used effectively in quantifying the distribution of species in solution.

Aquo and Hydroxo Complexes of (TSPP)Rh(III). A convenient entry point into the chemistry of water-soluble rhodium porphyrin species is through the hydrated rhodium(III) derivative of rhodium tetra *p*-sulfonatophenyl porphyrin ($Na_3[(TSPP)Rh(D_2O)_2]\cdot 18D_2O$ (**1**)). Dissolution of **1** in D_2O results in solutions of the bisaquo complex $[(TSPP)Rh^{III}(D_2O)_2]^{-3}$ (**2**) in an equilibrium distribution with the mono and bishydroxo complexes, $[(TSPP)Rh^{III}(D_2O)(OD)]^{-4}$ (**3**), $[(TSPP)Rh^{III}(OD)_2]^{-5}$ (**4**) (eqs 1, 2).

$$[(TSPP)Rh^{III}(D_2O)_2]^{-3} \rightleftharpoons [(TSPP)Rh^{III}(D_2O)(OD)]^{-4} + D^+ \quad (1)$$

$$[(TSPP)Rh^{III}(D_2O)(OD)]^{-4} \rightleftharpoons [(TSPP)Rh^{III}(OD)_2]^{-5} + D^+ \quad (2)$$

Rapid interchange of hydrogens from coordinated water and hydroxide with the bulk solvent water ($T = 275-300$ K) results in a single set of mole fraction averaged porphyrin ^{1}H NMR resonances for the equilibrium distribution of **2**, **3**, and **4** (Figure 1, Table 1). The mole fraction averaged pyrrole proton resonance for equilibrium distributions of **2**, **3**, and **4** as a function of the concentration of D^+ was used in determining the acid dissociation constants (298 K) for **2** ($K_1 = (1.4 \pm 0.2) \times 10^{-8}$) and **3** ($K_2 = (2.8 \pm 0.3) \times 10^{-12}$)[6] by nonlinear least-squares curve fitting to the equation: $\delta_{2,3,4(obs)}(pyr) = (K_1K_2\delta_4(pyr) + K_1[D^+]\delta_3(pyr) + [D^+]^2\delta_2(pyr))/(K_1K_2 + K_1[D^+] + [D^+]^2)$. The lower acidity for the D_2O complex **2** ($K_1(D_2O) = 1.4 \times 10^{-8}$) as compared to that of the previously studied H_2O derivative ($K_1(H_2O) = 9.67 \times 10^{-8}$)[15] parallels the smaller ion product constant for D_2O ($K_w(D_2O) = 1.35 \times 10^{-15}$) and ion dissociation constant ($K_3(D_2O) = 2.44 \times 10^{-17}$) as compared to those of H_2O ($K_w(H_2O) = 1.0 \times 10^{-14}$ and $K_3(H_2O) = 1.8 \times 10^{-16}$) at 298 K (Table 2, eq 3).

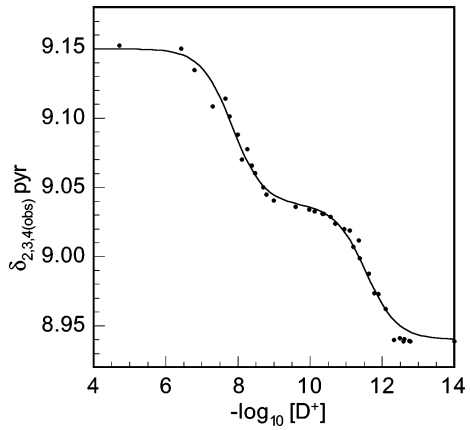

Figure 1. Data points are the observed limiting fast exchange mole fraction averaged pyrrole ^{1}H NMR chemical shifts for compounds **2**, **3**, and **4** in D_2O as a function of $-\log_{10}[D^+]$. The solid line is the nonlinear least-squares best fit line giving $K_1(298\ K) = (1.40 \pm 0.2) \times 10^{-8}$, $K_2(298\ K) = (2.8 \pm 0.3) \times 10^{-12}$, and $\delta_3(pyr) = 9.04$ ppm; **2** is $[(TSPP)Rh^{III}(D_2O)_2]^{-3}$, $\delta_2(pyr) = 9.15$ ppm; **4** is $[(TSPP)Rh^{III}(OD)_2]^{-5}$, $\delta_4(pyr) = 8.94$ ppm; **3** is $[(TSPP)Rh^{III}(D_2O)(OD)]^{-4}$.

Reactions of H_2/D_2 with Solutions of 1 in D_2O. The bis aquo complex $[(TSPP)Rh^{III}(D_2O)_2]^{-3}$ (**2**) reacts slowly with H_2/D_2 ($P_{H_2} \approx 0.5-0.8$ atm) in acidic D_2O media ($[D^+] > 10^{-5}$) to form complex **5** which is assigned as the hydride complex $[(TSPP)Rh-D(D_2O)]^{-4}$ (eq 4).

$$[(TSPP)Rh^{III}(D_2O)_2]^{-3} + D_2 \rightleftharpoons [(TSPP)Rh-D(D_2O)]^{-4} + D^+ + D_2O \quad (4)$$

(14) Subsequent papers in this series will focus on organometallic reactions of (TSPP)Rh−H and (TSPP)Rh−OH with CO, olefins, aldehydes, and ketones.

(15) Ashley K. R.; Shyu, S. B.; Leipoldt, J. G. *Inorg. Chem.* **1980**, *19*, 1613.

Table 2. The Measured Equilibrium Constants of (TSPP)Rh Reactions in D_2O ($T = 298$ K)[a]

(TSPP)Rh reactions	equilibrium constants K_n(298 K)	$\Delta G°$(298 K) kcal mol^{-1}
(1) $[Rh^{III}(D_2O)_2]^{-3} \rightleftharpoons [Rh^{III}(OD)(D_2O)]^{-4} + D^+$	$K_1 = (1.4 \pm 0.2) \times 10^{-8}$	$+10.7 \pm 0.1$
(2) $[Rh^{III}(OD)(D_2O)]^{-4} \rightleftharpoons [Rh^{III}(OD)_2]^{-5} + D^+$	$K_2 = (2.8 \pm 0.3) \times 10^{-12}$	$+15.8 \pm 0.1$
(3) $D_2O \rightleftharpoons OD^- + D^+$	$K_3 = 2.44 \times 10^{-17}$	$+22.6$[b]
(4) $[Rh^{III}(D_2O)_2]^{-3} + D_2 \rightleftharpoons [Rh{-}D(D_2O)]^{-4} + D^+ + D_2O$	$K_4 = 18.2 \pm 0.5$	-1.7 ± 0.1
(5) $[Rh{-}D(D_2O)]^{-4} \rightleftharpoons [Rh^{I}(D_2O)]^{-5} + D^+$	$K_5 = (8.0 \pm 0.5) \times 10^{-8}$	$+9.7 \pm 0.1$
(6) $[Rh^{III}(D_2O)_2]^{-3} + [Rh^{I}(D_2O)]^{-5} \rightleftharpoons [Rh^{II}(D_2O)]_2^{-8} + D_2O$	$K_6 = (2.3 \pm 0.5) \times 10^{5}$	-7.3 ± 0.1
(7) $D^+ + D^- \rightleftharpoons D_2$	$K_7 = 5.2 \times 10^{37}$	-53.2[c]

[a] The reported K values correspond to equilibrium constant expressions that contain all of the constituents given in the chemical equation including water. [b] The ion product of D_2O (14.869) and the D_2O density (1.1044) were used to determine that $K_3 = 2.44 \times 10^{-17}$ at 298 K. [c] $E°(2H^+ + 2e \rightleftharpoons H_2) = 0.00$ V and $E°(2H^- \rightleftharpoons H_2 + 2e) = +2.23$ V were used to evaluate $\Delta G°(H^+ + H^- \rightleftharpoons H_2) = -51.4$ kcal mol^{-1} and $\Delta G°(D^+ + D^- \rightleftharpoons D_2) = -53.2$ kcal mol^{-1}. *CRC Handbook of Chemistry and Physics*, 71st ed.; Lide, D. R., Ed.; CRC Press: Boca Raton, FL, 1990−1991; pp 8-38, 6-11, and 8-17.

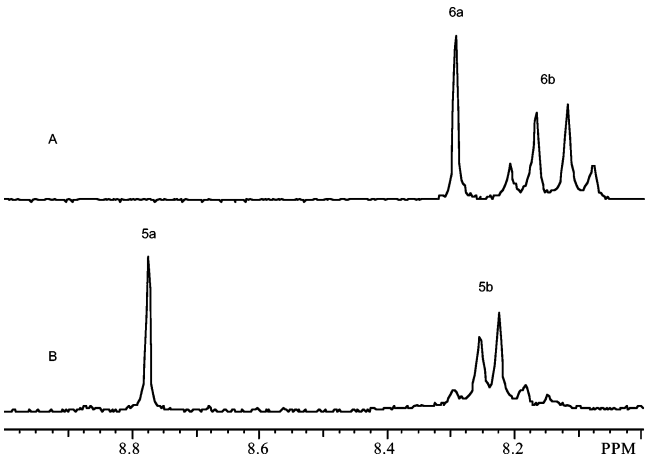

Figure 2. ^{1}H NMR (360 MHz) spectra in D_2O. (A) $[(TSPP)Rh^{I}(D_2O)]^{-5}$ (**6**) in D_2O, $[D^+] < 10^{-10}$ M, $T = 298$ K; (B) $[(TSPP)Rh{-}D(D_2O)]^{-4}$ (**5**), $[D^+] < 10^{-4}$ M, $T = 360$ K. a, pyrrole hydogens; b, phenyl hydrogens.

Reaction 4 achieves a conveniently measurable equilibrium distribution of species. The equilibrium constant for reaction 4 (K_4(298 K) $= 18.2 \pm 0.5$) was evaluated from the ^{1}H NMR studies in combination with D^+ concentration measurements and the solubility of D_2 in water.[16] Formation of the hydride complex **5** from reaction of H_2 in H_2O with **2** followed by removal of water and dissolution in DMF-d_6 results in the observation of a characteristic hydride ^{1}H NMR resonance ($\delta_{Rh-H} = -38$ ppm; $J_{Rh-H} = 31$ Hz) and an ABCD porphyrin phenyl resonance pattern associated with a static Rh−H unit that produces inequivalence of the porphyrin faces. This behavior contrasts with that of solutions of **5** in water and methanol where the hydride hydrogen rapidly exchanges as a proton with solvent hydroxylic hydrogens.

Solutions of **1** in basic media ($[D^+] \approx 10^{-8}-10^{-11}$ M), where the (TSPP)Rh(III) mono and bis hydroxo complexes **3** and **4** predominate, give a much faster reaction with H_2/D_2 than was observed for **2** and result in the formation of a rhodium(I) complex, $[(TSPP)Rh^{I}(D_2O)]^{-5}$ (**6**). The relatively high field ^{1}H NMR positions for the porphyrin pyrrole (δ_6(pyr) $= 8.32$ ppm) and phenyl hydrogens ($\delta_{o,o'} = 8.20$ ppm, $\delta_{m,m'} = 8.11$ ppm) observed for **6** are characteristic of the electron-rich metal site in rhodium(I) tetraphenyl porphyrin derivatives (Figure 2A, Table 1).[17] The AA′BB′ phenyl proton pattern which is observed for **5** throughout the convenient temperature range for water (275−350 K) is consistent with the porphyrin macrocycle being an effective plane of symmetry as expected for a rhodium(I) complex (Figure 2B). Reactions of (TSPP)Rh(III) complexes (**2**, **3**, **4**) in D_2O with an excess of $NaBD_4$ produce a species in solution with a ^{1}H NMR spectrum identical to that of **6** and thus is assigned as the rhodium(I) complex, $[(TSPP)Rh^{I}(D_2O)]^{-5}$.

Solutions of **6** in D_2O react rapidly with CH_3I exclusively to form a rhodium methyl derivative $[(TSPP)Rh{-}CH_3(D_2O)]^{-4}$ which is a signature reaction of the nucleophilic rhodium(I) center in **6**. The Rh−CH_3 complex is recognized easily in D_2O by the characteristic high field ^{1}HNMR methyl resonance (δ_6-(CH_3) $= -6.59$ ppm). The Rh−CH_3 unit results in an inequivalence of the porphyrin faces which is manifested by an ABCD ^{1}H NMR porphyrin phenyl resonance pattern like that observed for the hydride **5** in DMF. Spectroscopic and reactivity studies clearly identify **6** as the rhodium(I) derivative, $[(TSPP)Rh^{I}(D_2O)]^{-5}$. The reactivity of the Rh(I) complex (**6**) is not strongly influenced by the solvent donor properties because the 16-electron fragment species $[(TSPP)Rh^{I}]^{-5}$ resists addition of more than one donor molecule.

Acid Dissociation Constant of $[(TSPP)Rh{-}D(D_2O)]^{-4}$. Protonation of $[(TSPP)Rh^{I}(D_2O)]^{-5}$ (**6**) produces the rhodium hydride complex **5** by the reverse of eq 5.

$$[(TSPP)Rh{-}D(D_2O)]^{-4} \rightleftharpoons [(TSPP)Rh^{I}(D_2O)]^{-5} + D^+ \quad (5)$$

Aqueous solutions that contain both **5** and **6** manifest a single mole fraction averaged ^{1}H NMR spectrum that is a result of rapid proton interchange. A plot of $\delta_{5,6(obs)}$(pyr) for the equilibrium distribution of **5** and **6** in D_2O at a series of hydrogen ion (D^+) concentrations is illustrated in Figure 3. The mole fraction averaged pyrrole proton resonances ($\delta_{5,6(obs)}$(pyr)), as a function of the molar concentration of D^+, were used to determine the acid dissociation constant for the hydride **5** at 298 K ($K_5 = (8.0 \pm 0.5) \times 10^{-8}$) by nonlinear least-squares curve fitting to the relationship: $\delta_{5,6(obs)}(pyr) = (K_5\delta_6(pyr) + [D^+]\delta_5(pyr))/(K_5 + [D^+])$.

Formation of a $Rh^{II}-Rh^{II}$ Bonded Species in D_2O. Mixing D_2O solutions of $[(TSPP)Rh^{III}(D_2O)_2]^{-3}$ (**2**) with solutions containing the $[(TSPP)Rh^{I}(D_2O)]^{-5}$ complex (**6**) results in an equilibrium distribution with a $Rh^{II}-Rh^{II}$ bonded dimer, $[(TSPP)Rh^{II}(D_2O)]_2^{-8}$ (**7**) (eq 6, Figure 4).

$$[(TSPP)Rh^{III}(D_2O)_2]^{-3} + [(TSPP)Rh^{I}(D_2O)]^{-5} \rightleftharpoons [(TSPP)Rh^{II}(D_2O)]_2^{-8} + D_2O \quad (6)$$

The equilibrium constant at 298 K for the formation of $[(TSPP)Rh^{II}(D_2O)]_2^{-8}$ from the bisaquo complex **2** and rhodium-

(16) Fog, P. G. T.; Gerrard, W. *Solubility of Gases In Liquids: A Critical Evaluation of Gas/Liquid Systems in Theory and Practice*; Wiley: Chichester, NY, 1991.
(17) Wayland, B. B.; Van Voorhees, S. L.; Wilker, C. *Inorg. Chem.* **1986**, *25*, 4039.

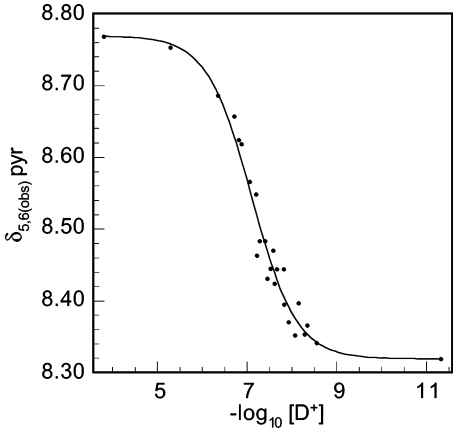

Figure 3. Data points are the fast exchange mole fraction averaged ^{1}H NMR chemical shifts for [(TSPP)Rh−D(D$_2$O)]$^{-4}$ (**5**) and [(TSPP)Rh^I(D$_2$O)]$^{-5}$ (**6**) in D$_2$O as a function of $-\log_{10}[D^+]$. The solid line is the nonlinear least-squares best fit line giving $K_5(298\ K) = (8.0 \pm 0.5) \times 10^{-8}$, $\delta_5(pyr) = 8.78$ ppm, $\delta_6(pyr) = 8.32$ ppm.

(I) complex **6** depicted by reaction 6 ($K_6 = [\mathbf{7}][D_2O]/([\mathbf{2}][\mathbf{6}]) = (2.3 \pm 0.5) \times 10^5$) was determined from the ^{1}H NMR chemical shifts and intensities in combination with equilibrium constants determined for the equilibria involving **2** with **3** (eq 1) and **5** with **6** (eq 5). The Rh^{II}−Rh^{II} bonded dimer **7** is observed as a prominent species only when the solution is close to neutrality ([D$^+$] ≈ 10^{-8}−10^{-7}), and **7** is not observed in the ^{1}H NMR spectra in acidic ([D$^+$] > 10^{-5}) or basic ([D$^+$] < 10^{-10}) solutions.

The Rh^{II}−Rh^{II} bonded dimer (**7**) is readily identified in solution by comparison of the distinctive porphyrin ^{1}H NMR spectrum of **7** (Figure 4) with previously reported NMR spectra for [(por)Rh^{II}]$_2$ complexes[17] and other metal−metal bonded face-to-face dimers.[18] ^{1}H NMR shifts of the four sets of phenyl hydrogens in monoporphyrin (TSPP)Rh complexes occur within a small range ($\delta = 8.3 \pm 0.2$ ppm), but in the diporphyrin complex **7** they occur over a range of 2.5 ppm ($\delta = 9.5$−7.0 ppm) (Figure 4). The magnetic field from the combined ring currents of adjacent porphyrin rings produces an exceptionally large downfield shift for the ortho phenyl hydrogens (δ_7(ortho) = 9.5 ppm) that are situated between the porphyrin rings and an unusually high field position for the exterior ortho phenyl hydrogens (δ_7(ortho) = 7.0 ppm). The exceptionally low field peak positions for the ortho phenyl hydrogens that occur between the porphyrin rings are uniquely characteristic of metal−metal bonded dimers of tetraphenyl porphyrin derivatives. The ortho phenyl hydrogens that are directed between the two porphyrin planes experience the combined deshielding ring current effects associated with the periphery of the aromatic rings, and the resulting unique low field position for these hydrogens in the ^{1}H NMR spectrum is an unmistakable signature for a face-to-face diporphyrin structure (Figure 4). The relatively high field position for the pyrrole hydrogens of **7** (δ_7(pyr) = 8.46 ppm) is another characteristic feature of the ^{1}H NMR spectrum of **7** that is shared with [(TPP)Rh^{II}]$_2$.[17]

The Rh^{II}−Rh^{II} bonded dimer (**7**) is also observed along with Rh(III) and Rh(I) species in the photolysis (λ > 350 nm) of [(TSPP)Rh−CH$_3$(D$_2$O)]$^{-4}$ in neutral D$_2$O solution. When the [D$^+$] is less than 10^{-8} ([D$^+$] < 10^{-8}), photolysis of [(TSPP)Rh−CH$_3$(D$_2$O)]$^{-4}$ gives the Rh(I) complex **6** exclusively, and in acidic solution ([D$^+$] > 10^{-4}), only the bisaquo Rh(III) species **2** is observed. The initial photo process probably results in Rh−CH$_3$ bond homolysis to produce a (TSPP)Rh^{II} species that dimerizes to **7**. The Rh^{II}−Rh^{II} bonded complex **7** disproportionates by the reverse of reaction 6 into an equilibrium distribution of **7** with rhodium(III) and rhodium(I) species in D$_2$O.

The qualitative relationships between the (TSPP)Rh species (Rh(III), Rh(II), Rh(I), Rh−D) in D$_2$O are summarized by the pentagon shown in Scheme 1. Experimentally measured quantitative relationships between the solution species **2**−**7** depicted by eqs 1−7 are summarized in Table 2.

Discussion

Reactions of (TSPP)Rh(III) aquo and hydroxo species with dihydrogen in water produce a series of equilibria where the equilibrium constants have been directly evaluated (Table 2). In aqueous solution, the equilibrium distributions for all of the (TSPP)Rh reaction precursor species, Rh^{III}, Rh^I, Rh−D, and Rh^{II}, are either directly or indirectly dependent on the hydrogen ion concentration ([D$^+$]). Variation of the hydrogen ion concentration provides an effective method for controlling the equilibrium distribution of (TSPP)Rh species in water that is not available in organic solvent media. The hydrogen ion concentration determines the distribution of the bisaquo complex (**2**) with the mono and bis hydroxo species (**3**, **4**), which in turn influences the distribution of product species at equilibrium. Reactions of (TSPP)Rh^{III} species (**2**, **3**, **4**) with H$_2$/D$_2$ in D$_2$O are prime examples where both the fraction of conversion for Rh(III) species (eqs 4, 8, 9) and the distribution of Rh−D and Rh^I products (eq 5) are dependent on the concentration of D$^+$.

$$[(TSPP)Rh^{III}(OD)(D_2O)]^{-4} + D_2 \rightleftharpoons [(TSPP)Rh{-}D(D_2O)]^{-4} + D_2O \quad (8)$$

$$[(TSPP)Rh^{III}(OD)_2]^{-5} + D_2 \rightleftharpoons [(TSPP)Rh^{I}(D_2O)]^{-5} + D_2O \quad (9)$$

The extent of conversion of the Rh(III) species depends on the distribution of aquo and hydroxo species that is described by eqs 1 and 2, while the distribution of the hydride (**5**) and Rh(I) complex (**6**) is determined by the acid dissociation constant of $(8.0 \pm 0.5) \times 10^{-8}$ for [(TSPP)Rh−D(D$_2$O)]$^{-4}$ (eq 5). In basic solution ([D$^+$] < 10^{-8}), high conversion to [(TSPP)Rh^I(D$_2$O)]$^{-5}$ (**6**) occurs, while in acidic media, the hydride [(TSPP)Rh−D(D$_2$O)]$^{-4}$ is the dominant species, but the extent of conversion for Rh(III) is lower (eq 4).

Equilibrium constants for a series of reactions including reactions 8 and 9 that are derived from measured K values for reactions 1−7 are given in Table 3 ($K_8 = K_1^{-1}K_4 = 1.3 \times 10^9$; $\Delta G_8° = -12.4$ kcal mol^{-1}; $K_9 = K_1^{-1}K_2^{-1}K_4K_5 = 3.6 \times 10^{13}$; $\Delta G_9° = -18.5$ kcal mol^{-1}). The large negative values for $\Delta G_8°$ and $\Delta G_9°$ illustrate that the reactions of H$_2$/D$_2$ with (TSPP)Rh^{III} species are much more thermodynamically favorable for the hydroxo species **3** and **4** as compared to the bisaquo complex **2**. The acidic condition needed to give high conversion of the Rh^I complex **6** to the hydride complex **5** (eq 5) is also associated with the presence of [(TSPP)Rh^{III}(D$_2$O)$_2$]$^{-3}$ by the reverse of reaction 4. Stable equilibrium concentrations of the hydride (**5**) require the presence of H$_2$/D$_2$ to achieve equilibrium with the

(18) Collman, J. P.; Barnes, C. E.; Collins, T. J.; Brothers, P. J. *J. Am. Chem. Soc.* **1981**, *103*, 7030.

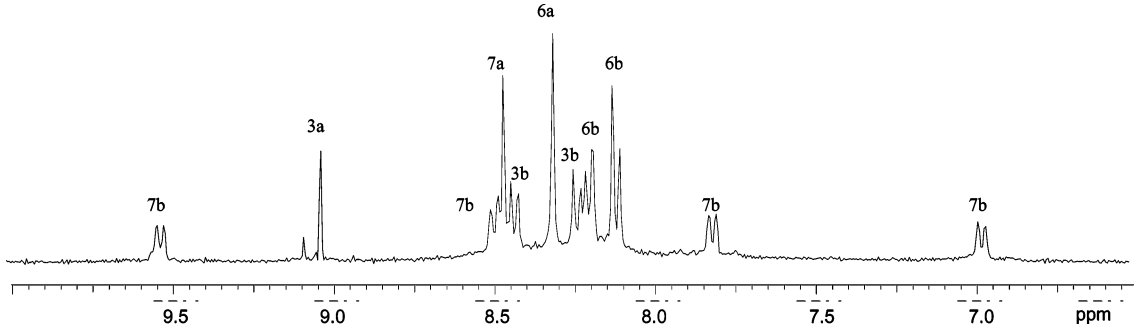

Figure 4. ^{1}H NMR (360 MHz) spectrum of $[(TSPP)Rh^{II}(D_2O)]_2^{-8}$ (**7**) in equilibrium with $[(TSPP)Rh^{I}]^{-5}$ (**6**) and (TSPP)Rh(III) species **2** and **3** in D_2O ($[D^+] = 10^{-8}$ M), where a and b designated the pyrrole and phenyl hydrogens, respectively, in species **3**, **6**, and **7**.

Scheme 1. The (TSPP)Rh Species in Simultaneous Multiple Equilibria in Water

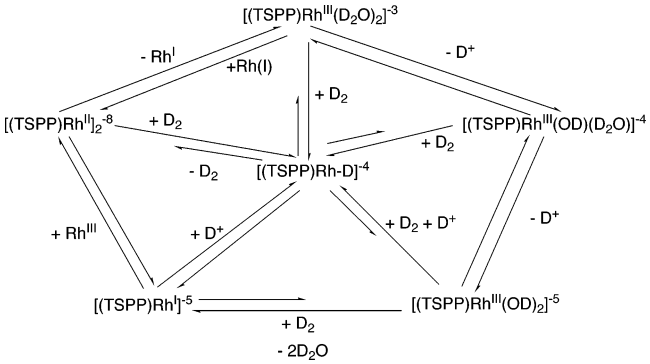

Rh(III) complexes (**2**, **3**, **4**) (eq 4) and maintain the simultaneous multiple equilibria with the Rh−D and Rh(I) species (**5**, **6**).

When Rh(III) and Rh(I) species are simultaneously present in aqueous solution, then a $Rh^{II}-Rh^{II}$ bonded dimer(II) also occurs in accord with reaction 6 (K_6(298 K) = (2.3 ± 0.5) × 10^5). Compound **7** can be viewed as resulting from the nucleophilic Rh(I) center sharing the pair of d_{z2} electrons with the empty d_{z2} on the Rh(III) species (Rh^I: → Rh^{III}). The $Rh^{II}-Rh^{II}$ bonded dimer $[(TSPP)Rh^{II}(D_2O)]_2^{-8}$ (**7**) achieves ^{1}H NMR observable concentrations at near neutral conditions where the rhodium(III) bisaquo complex (**2**) and the rhodium(I) complex (**6**) occur together. Although production of $[(TSPP)Rh^{II}(D_2O)]_2^{-8}$ by reaction 6 is not directly dependent on the $[D^+]$, the fraction of (TSPP)Rh species in solution that are in equilibrium with **7** are highly sensitive to the $[D^+]$. The quantity of $Rh^{II}-Rh^{II}$ bonded dimer (**7**) that occurs at equilibrium becomes small at both high and low $[D^+]$ because the conversion of the rhodium(I) complex (**6**) to the hydride (**5**) occurs at high $[D^+]$ and conversion of the Rh(III) bisaquo complex (**2**) to the mono and bis hydroxo complexes (**3**, **4**) occurs at low $[D^+]$ (eqs 10, 11).

$$[(TSPP)Rh^{II}(D_2O)]_2^{-8} + D^+ + D_2O \rightleftharpoons [(TSPP)Rh-D(D_2O)]^{-4} + [(TSPP)Rh^{III}(D_2O)_2]^{-3} \quad (10)$$

$$[(TSPP)Rh^{II}(D_2O)]_2^{-8} + OD^- \rightleftharpoons [(TSPP)Rh^{I}(D_2O)]^{-5} + [(TSPP)Rh-OD(D_2O)]^{-4} \quad (11)$$

Equilibrium constants (298 K) for reaction 10 derived from measured K values for reactions 1, 3, 5, and 6 ($K_{10} = K_5^{-1}K_6^{-1}$ = 54) and 11 ($K_{11} = K_6^{-1}K_1K_3^{-1} = 2.4 \times 10^3$) show that reactions of **7** with both D^+ and OD^- in D_2O are thermodynamically favorable.

Thermodynamics for Displacement of a Water Molecule from $[(TSPP)Rh^{III}(D_2O)_2]^{-3}$ by $[(TSPP)Rh^{I}(D_2O)]^{-5}$, Hydroxide ($OD^-$), and Hydride ($D^-$). Equilibrium constants and standard free energy changes for displacement of water (D_2O) from the rhodium(III) center in **2** ($[(TSPP)Rh^{III}(D_2O)_2]^{-3}$) by the rhodium(I) complex (**6**) (eq 6), hydroxide (OD^-) (eq 12), and hydride (D^-) (eq 13) are either directly measured (eq 6, Table 2) or derived from measured thermodynamic values for reactions 1−7 (eqs 12, 13; Table 3).

$$[(TSPP)Rh^{III}(D_2O)_2]^{-3} + OD^- \rightleftharpoons [(TSPP)Rh-OD(D_2O)]^{-4} + D_2O \quad (12)$$

$$[(TSPP)Rh^{III}(D_2O)_2]^{-3} + D \rightleftharpoons [(TSPP)Rh-D(D_2O)]^{-4} + D_2O \quad (13)$$

The rhodium(I) complex ($[(TSPP)Rh^{I}(D_2O)]^{-5}$) functions as a metal-centered nucleophile through use of the pair of electrons in d_{z2} (Rh^I:). Substitution of $[(TSPP)Rh^{I}(D_2O)]^{-5}$ for D_2O in **2** produces an equilibrium with the $Rh^{II}-Rh^{II}$ bonded dimer ($[(TSPP)Rh^{II}(D_2O)]_2^{-8}$) **7** that has been directly evaluated (eq 6, K_6(298 K) = (2.3 ± 0.5) × 10^5, $\Delta G_6°$(298 K) = −7.3 kcal mol^{-1}). Substitution of hydroxide (OD^-) and hydride (D^-) for water is derived from reactions 1 and 3 ($\Delta G_{12}° = \Delta G_1° - \Delta G_3°$ = −11.9 kcal mol^{-1}) and reactions 4 and 7 ($\Delta G_{13}° = \Delta G_4° + \Delta G_7°$ = −54.9 kcal mol^{-1}), respectively. The free energy changes for reactions 6, 12, and 13 ($\Delta G_6°$, $\Delta G_{12}°$, $\Delta G_{13}°$) correspond to differences in the heterolytic BDFE value for $Rh^{III}-X$ (X = OD^-, D^-, Rh^I) in complexes **3**, **5**, **7**, and the $Rh^{III}(D_2O)$ BDFE in **2**. Each of these water displacement reactions is highly favorable, but hydride stands out as an exceptionally strong donor ($\Delta G_{13}° = -54.9$ kcal mol^{-1}).

The Bond Dissociation Free Energy (BDFE) Difference between Rh−OD and Rh−D. The difference in Rh−OD and Rh−D bond dissociation free energies can be obtained by using reaction 8 ($[(TSPP)Rh^{III}-OD(D_2O)]^{-4} + D_2 \rightleftharpoons [(TSPP)Rh-D(D_2O)]^{-4} + D_2O$). Reaction 8 is an example process that effectively occurs to completion at the attainable range of experimental conditions and thus could not be directly determined. Combining reaction 4 with the reverse of reaction 1 results in reaction 8, and the derived equilibrium constant K_8 is given by K_4/K_1 ($K_8 = K_4/K_1 = 1.3 \times 10^9$; $\Delta G_8° = -12.4$ kcal mol^{-1}). The difference in the $(Rh-OD)_{aq}$ and $(Rh-D)_{aq}$ bond dissociation free energies (BDFE) can be derived by expressing $\Delta G_8°$ in terms of a BDFE for each bond formed or broken in reaction 8 ($\Delta G_8° = -12.4$ kcal mol^{-1} = $(Rh-OD)_{aq}$ +

Table 3. Equilibrium Constants (298 K) for (TSPP)Rh Reactions Derived from Reactions in Table 2[a]

derived (TSPP)Rh reactions	equilibrium constants K_n(298 K)	$\Delta G°$(298 K) kcal mol^{-1}
(8) $[Rh^{III}(OD)(D_2O)]^{-4} + D_2 \rightleftharpoons [Rh-D(D_2O)]^{-4} + D_2O$	$K_8 = K_1^{-1}K_4 = 1.3 \times 10^9$	-12.4 ± 0.1
(9) $[Rh^{III}(OD)_2]^{-5} + D_2 \rightleftharpoons [Rh^{I}(D_2O)]^{-5} + D_2O$	$K_9 = K_1^{-1}K_2^{-1}K_4K_5 = 3.6 \times 10^{13}$	-18.5
(10) $[Rh^{II}(D_2O)]_2^{-8} + D^+ + D_2O \rightleftharpoons [Rh-D(D_2O)]^{-4} + [Rh^{III}(D_2O)_2]^{-3}$	$K_{10} = K_5^{-1}K_6^{-1} = 54$	-2.4 ± 0.1
(11) $[Rh^{II}(D_2O)]_2^{-8} + OD^- \rightleftharpoons [Rh^{I}(D_2O)]^{-5} + [Rh^{III}(OD)(D_2O)]^{-4}$	$K_{11} = K_6^{-1}K_1K_3^{-1} = 2.4 \times 10^3$	-4.6 ± 0.1
(12) $[Rh^{III}(D_2O)_2]^{-3} + OD^- \rightleftharpoons [Rh-OD(D_2O)]^{-4} + D_2O$	$K_{12} = K_1K_3^{-1} = 5.7 \times 10^8$	-11.9 ± 0.1
(13) $[Rh^{III}(D_2O)_2]^{-3} + D^- \rightleftharpoons [Rh-D(D_2O)]^{-4} + D_2O$	$K_{13} = K_4K_7 = 2.0 \times 10^{41}$	-54.9
(14) $[Rh^{II}(D_2O)]_2^{-8} + D_2 \rightleftharpoons 2[Rh-D(D_2O)]^{-4}$	$K_{14} = K_4K_5^{-1}K_6^{-1} = 9.8 \times 10^2$	-4.1 ± 0.1
(15) $[Rh^{III}(D_2O)]_2^{-8} + D_2O \rightleftharpoons [Rh-D(D_2O)]^{-4} + [Rh-OD(D_2O)]^{-4}$	$K_{15} = K_1K_5^{-1}K_6^{-1} = 7.5 \times 10^{-7}$	$+8.4 \pm 0.1$

[a] The reported K values correspond to equilibrium constant expressions that contain all of the constituents given in the chemical equation including water.

Table 4. Summary of $\Delta H°$ and $\Delta G°$(298 K) for Bond Homolysis of H−H, D−D, H−OH, and D−OD[a]

X–Y → X• + Y•	BDFE kcal mol^{-1}	BDE kcal mol^{-1}
$H-H_g$	97.1	104.2
$H-H_{aq}$	101.8	103.2
$D-D_g$	98.7	105.9
$D-D_{aq}$	103.4	104.5
$H-OH_g$	112.0	118.8
$H-OH_{aq}$	116.1	123.5
$D-OD_g$	113.5	120.3
$D-OD_{aq}$	117.6	124.8

[a] See the Experimental Section for the analysis of $\Delta H°$ and $\Delta G°$(298 K) for bond homolysis of H−H, D−D, H−OH, and D−OD in water.

$(D-D)_{aq} - (Rh-D)_{aq} - (D-OD)_{aq}$; $((Rh-OD)_{aq} - (Rh-D)_{aq}) = -12.4 - (D-D)_{aq} + (D-OD)_{aq} = -12.4 - 103.4 + 117.6 = 1.8$ kcal mol^{-1}). The difference of ~1.8 kcal mol^{-1} between the $(Rh-OD)_{aq}$ and $(Rh-D)_{aq}$ BDFE should be highly reliable because it is based on equilibrium measurements that give $\Delta G°$ values that are accurate within 0.1 kcal mol^{-1} (Tables 2, 3) and well-established thermodynamic values for D_2 and D_2O in the gas phase and in aqueous solution (Table 4).

Equilibrium studies relevant to transition metal-hydride homolytic dissociation are quite rare. The studies most closely analogous to those reported here are displacement equilibria in THF for $Cp*(PMe_3)_2Ru-OH$ with H_2 to form $Cp*(PMe_3)_2Ru-H$ and H_2O which were used to generate a scale of relative homolytic bond dissociation energies including both Ru−OH and Ru−H.[19] The difference of the Ru−OH and Ru−H BDFE was found to be ~9 kcal mol^{-1},[19] which is much larger than the observed difference for the (TSPP)Rh hydroxo and hydride complexes in water ($(Rh-OD) - (Rh-D) \approx 1.8$ kcal mol^{-1}; $(Rh-OH) - (Rh-H) \approx 2.8$ kcal mol^{-1}). The smaller difference in M−OH and M−H BDFE in water may reflect differences in the solvation energies of H• and •OH in water that result from water being a more highly structured medium than THF. The difference between the free energy for hydration of •OH and H• is ~7 kcal mol^{-1} ($\Delta G°_{hyd}(H•)(298\ K) = +4.5$ kcal mol^{-1}; $\Delta G°_{hyd}(•OH)(298\ K) = -2.4$ kcal mol^{-1}),[25a,b] which could be responsible for most of the difference in the $((Rh-OH) - (Rh-H))$ BDFE observed in water as compared to that in THF.

Substrate reactions of $[(TSPP)Rh^{II}]_2^{-8}$ with hydrogen (eq 14) and water (eq 15) that describe Rh−D and Rh−OD homolysis processes are derived from reactions 1 and 4−6 ($K_{14} = K_4/K_5K_6 = 9.8 \times 10^2$, $\Delta G_{14}° = -4.1$ kcal mol^{-1}; $K_{15} = K_1/K_5K_6 = 7.5 \times 10^{-7}$; $\Delta G_{15}° = +8.4$ kcal mol^{-1}).

$$[(TSPP)Rh^{II}(D_2O)]_2^{-8} + D_2 \rightleftharpoons 2[(TSPP)Rh-D(D_2O)]^{-4} \quad (14)$$

$$[(TSPP)Rh^{II}(D_2O)]_2^{-8} + D_2O \rightleftharpoons [(TSPP)Rh-D(D_2O)]^{-4} + [(TSPP)Rh^{III}-OD(D_2O)]^{-4} \quad (15)$$

Expressing $\Delta G_{14}°$ as a series of BDFE terms ($\Delta G_{14}° = -4.1$ kcal mol^{-1} $= (Rh-Rh)_{aq} + (D-D)_{aq} - 2(Rh-D)_{aq}$) shows that evaluation of the absolute rhodium−hydride ($(Rh-D)_{aq}$) BDFE and rhodium hydroxide ($(Rh-OD)_{aq}$) in water requires determining the $(Rh-Rh)_{aq}$ BDFE ($(Rh-D)_{aq}$ BDFE = 53.8 kcal mol^{-1} + $^1/_2(Rh-Rh)_{aq}$ BDFE). Reaction 15 describes the homolysis of water by the $Rh^{II}-Rh^{II}$ species which is thermodynamically unfavorable ($\Delta G_{15}° = +8.4$ kcal mol^{-1}) because of the $Rh^{II}-Rh^{II}$ BDFE.

$Rh^{II}-Rh^{II}$ Heterolysis and Estimated Homolysis Energetics. Heterolytic bond cleavage of the $Rh^{II}-Rh^{II}$ bonded dimer $[(TSPP)Rh^{II}(D_2O)]_2^{-8}$ (**7**) to form $[(TSPP)Rh^{III}(D_2O)_2]^{-3}$ (**2**) and $[(TSPP)Rh^{I}(D_2O)]^{-5}$ (**6**) was directly measured by the reverse of reaction 6 ($[(TSPP)Rh^{II}(D_2O)]_2^{-8} + D_2O \rightleftharpoons [(TSPP)Rh^{III}(D_2O)_2]^{-3} + [(TSPP)Rh^{I}(D_2O)]^{-5}$; $K_6^{-1} = (2.4 \pm 0.3) \times 10^{-4}$; $\Delta G_6°^{-1}(298\ K) = +7.3 \pm 0.1$ kcal mol^{-1}). Efforts to observe homolytic dissociation of the $Rh^{II}-Rh^{II}$ dimer into monomeric Rh(II) species were precluded because the lower energy heterolytic dissociation into ions is virtually complete before achieving a temperature where the ^{1}H NMR line broadening as chemical shifts from the higher activation energy bond homolysis process would be observed. The inability to measure a $Rh^{II}-Rh^{II}$ bond homolysis free energy and enthalpy for **7** prohibits an entirely experimental evaluation of the Rh−D BDFE in **5** and the Rh−OD BDFE in **3**.

^{1}H NMR line broadening for the rhodium(II) dimers of octaethylporphyrin and tetraphenyl porphyrin in benzene was previously used in deriving $Rh^{II}-Rh^{II}$ bond homolysis activation enthalpies and estimation of the homolysis enthalpy in the range of 16−18 kcal mol^{-1}.[20] Aquation of these weak acceptor species should not differ greatly, and thus the $Rh^{II}-Rh^{II}$ bond homolysis energy is expected to be comparable to those in benzene ($\Delta H° \approx$

(19) Bryndza, H. E.; Fong, L. K.; Paciello, R. A.; Tam, W.; Bercaw, J. E. *J. Am. Chem. Soc.* **1987**, *109*, 1444.
(20) Wayland, B. B.; Coffin, V. L.; Farnos, M. D. *Inorg. Chem.* **1988**, *27*, 2745.
(21) Kristjansdottir, S. S.; Norton, J. R. In *Transition Metal Hydrides*; Dedieu, A., Ed.; VCH: New York, 1992; Chapter 9, pp 316−323.
(22) (a) Ellis, W. W.; Miedaner, A.; Curtis, C. J.; Gibson, D. H.; DuBois, D. L. *J. Am. Chem. Soc.* **2002**, *124*, 1926. (b) Curtis, C. J.; Miedaner, A.; Ellis, W. W.; DuBois, D. L. *J. Am. Chem. Soc.* **2002**, *124*, 1918.
(23) Values obtained from: *J. Phys. Chem. Ref. Data* **1982**, *11*, supplement 2. Standard state used: 298.15 K, 0.1 MPa.
(24) Blanksby, S. J.; Ellison, G. B. *Acc. Chem. Res.* **2003**, *36*, 255.
(25) (a) Han, P.; Bartels, D. M. *J. Phys. Chem.* **1990**, *94*, 7294. (b) Schwarz, H.; Dodson, R. W. *J. Phys. Chem.* **1984**, *88*, 3643. (c) Hamad, S.; Lago, S.; Mejias, J. A. *J. Phys. Chem. A* **2002**, *106*, 9104.

18 kcal mol^{-1}; $\Delta G° \approx 10-14$ kcal mol^{-1}). The preliminary estimate of 60 ± 3 kcal mol^{-1} for the $(Rh-D)_{aq}$ BDFE is made from an estimation of 12 ± 3 kcal mol^{-1} for the $Rh^{II}-Rh^{II}$ BDFE in water.

Proton, Hydrogen Atom, and Hydride Donor Energetics for (TSPP)Rh−D in Water. The acid dissociation constant for the hydride $[(TSPP)Rh-D(D_2O)]^{-4}$ was directly evaluated as $(8.0 \pm 0.5) \times 10^{-8}$ in water ($K_5(298\ K) = (8.0 \pm 0.5) \times 10^{-8}$; $\Delta G_5°(298\ K) = 9.7 \pm 0.1$ kcal mol^{-1}). The hydride **5** is somewhat more acidic than most metal hydrides,[21] and the pK_a falls between the values for the rhodium hydride derivatives of tetraphenyl porphyrin (pK_a = 11) and the perfluorinated derivative (pK_a= 2.1) measured in DMSO.[4] Displacement of hydride (D^-) from **5** by D_2O occurs with a $\Delta G°$ of 54.9 kcal mol^{-1}, and this free energy change is called the hydricity[22] of **5**. The Rh−D BDFE to produce a hydrogen atom (60 kcal mol^{-1}) and the heterolysis process to produce a hydride (54.9 kcal mol^{-1}) are both very high energy processes as compared to proton donation ($\Delta G°(298\ K) = 9.7 \pm 0.1$ kcal mol^{-1}). Acid dissociation of the rhodium hydride complex provides a facile source of rhodium(I) species with an accessible site for substrate reactions at the nucleophilic rhodium(I) center.

Summary

Reactions of (TSPP)Rh(III) aquo and hydroxo complexes with H_2/D_2 in D_2O result in simultaneous multiple equilibria involving Rh−D, Rh(I), Rh(II), and Rh(III) species. Equilibrium thermodynamic relationships between the (TSPP)Rh species in D_2O are described by a set of experimentally determined equilibrium constants (298 K) (Table 2). The hydrogen ion ($[D^+]$) dependence of the reactions in D_2O was used to establish distributions of species appropriate to measure solution equilibria using ^{1}H NMR spectroscopy and to identify conditions where specific species are dominant. The hydride complex (Rh−D) **5** functions as a weak acid in water (D_2O) ($K_a = 8.0 \times 10^{-8}$) and is thus a facile source of the rhodium(I) complex **6**. Thermodynamic parameters for the directly observed reactions were used in the derivation of thermodynamic values for a series of reactions where the equilibrium constants were either too small or too large to be directly evaluated. The difference between the $(Rh-D)_{aq}$ BDFE in **5** and the $(Rh-OD)_{aq}$ BDFE in **3** is determined to be small ($\sim +1.8$ kcal mol^{-1}), and the (Rh−D) BDFE is estimated to be $\sim 60 \pm 3$ kcal mol^{-1}. Each of the (TSPP)Rh species reported in this Article has a substantial scope of substrate organometallic reactivity, and the equilibrium studies reported in this Article establish a foundation for thermodynamic measurements for a wide array of substrate reactions in aqueous media.

Experimental Section

General Considerations. D_2O was purchased from Cambridge Isotope Laboratory Inc. and degassed by three freeze−pump−thaw cycles before use. Tetra *p*-sulfonatophenyl porphyrin sodium salt was purchaced from Mid-Centurary Chemicals. Research grade hydrogen was purchased from Matheson Gas Products and used without further purification.

Proton NMR spectra were obtained on a Bruker AC-360 interfaced to an Aspect 300 computer at ambient temperature. Chemical shifts were referenced to 3-trimethylsilyl-1 propanesulfonic acid sodium salt. Proton NMR spectra was used to identify solution species and to determine the distribution of species at equilibrium. pH measurements are performed on an Orion model 410 plus pH meter and Orion 9802 electrode precalibrated by Thermo Orion buffer solutions of pH = 4.01, 7.00, and 10.01.

$Na_3[(TSPP)Rh^{III}(D_2O)_2]$. $Na_3[(TSPP)Rh^{III}(D_2O)_2]$ was synthesized by literature methods of Ashley.[15] ^{1}H NMR (D_2O, 360 MHz) δ(ppm): 9.15 (s, 8H, pyrrole), 8.44 (d, 8H, *o*-phenyl, $J_{1H-1H} = 8$ Hz), 8.25 (d, 8H, *m*-phenyl, $J_{1H-1H} = 8$ Hz).

Concentration of Complexes and Ionic Strength of Aqueous Solutions. Thermodynamic studies of (TSPP)Rh complexes in water were carried out at concentrations less than 2×10^{-3} M to minimize molecular and ionic association. Most equilibrium constant measurements were performed at a low ionic strength ($\mu \approx 10^{-3}$) where the ion activity coefficients approach unity. Variation of the ionic strength in the low range where the Debye−Hückel equation pertains ($5 \times 10^{-4}-2 \times 10^{-2}$) did not perturb the spectroscopic parameters for the (TSPP)Rh species in D_2O or alter the measured acid dissociation constants beyond the reported error limits. High ionic strength ($\mu >$ 0.1) obtained by addition of $NaClO_4$ produces significant changes in the ^{1}H NMR spectra for the (TSPP)Rh solution species which may be associated with both ion pairing and ionic competing with water for coordination of the rhodium center.

$[(TSPP)Rh-D]^{-4}$ (5)/$[(TSPP)Rh^{I}]^{-5}$ (6). First, 0.3 mL of $[(TSPP)Rh^{III}(D_2O)_2]^{-3}$ D_2O stock solutions ($(1.2-1.8) \times 10^{-3}$ M, $[D^+] > 10^{-5}$ M) was added into a vacuum adapted NMR tube. H_2/D_2 (300−500 Torr) was pressurized into the NMR tube after three freeze−pump−thaw cycles, and the tube was flame-sealed. The reaction of **2** with H_2/D_2 producing **5** in acidic solution achieves equilibrium distributions of $(TSPP)Rh^{III}$ and $[(TSPP)Rh-D]^{-4}$ species within 2 months at 298 K. The equilibrium constant was evaluated from the intensity integrations of the ^{1}H NMR spectrum of each species in combination with the D^+ concentration measurement and the solubility of H_2/D_2 in water.[16] Following the same procedure, $(TSPP)Rh^{III}$ complexes completely converted to **6** in basic D_2O solution ($[D^+] < 10^{-10}$ M) in 7 days at 298 K. ^{1}H NMR (**5**) (D_2O, 360 MHz) δ (ppm): 8.78 (s, 8H, pyrrole), δ = 8.25 (s, 16H, phenyl). ^{1}H NMR (**6**) (D_2O, 360 MHz) δ (ppm): 8.32 (s, 8H, pyrrole), 8.20 (d, 8H, *o*-phenyl, $J_{1H-1H} = 8.2$ Hz), 8.11 (d, 8H, *m*-phenyl, $J_{1H-1H} = 8.2$ Hz).

$[(TSPP)Rh-Rh(TSPP)]^{-8}$ (7). Equal molar quantities of **6** and **2** in D_2O solution ($\sim 10^{-3}$ M) were mixed in a NMR tube in an inert atmosphere box, and the reaction reaches equilibrium in 24 h. ^{1}H NMR spectroscopy was used to determine the equilibrium distribution of Rh^{III} species including complex **2** and **3**, rhodium hydride **5**, rhodium(I) **6**, and rhodium(II) dimer **7**. The equilibrium constant of reaction 6 is evaluated from the intensity integration of each rhodium species in combination with equilibrium constants of eq 1 and 5 which determine the equilibrium distribution of rhodium complex **2** with **3** and **5** with **6**, respectively. ^{1}H NMR (**7**) (D_2O, 360 MHz) δ (ppm): 8.46 (s, pyrrole, 16H), 9.51 (d, 4H, *o*-phenyl, $J_{1H-1H} = 8$ Hz), 8.47 (d, 4H, *m*-phenyl, $J_{1H-1H} = 8$ Hz), 7.80 (d, 4H, *m*-phenyl, $J_{1H-1H} = 8$ Hz), 6.95 (d, 4H, *o*-phenyl, $J_{1H-1H} = 8$ Hz).

$[(TSPP)Rh-CH_3]^{-4}$. $[(TSPP)Rh-CH_3]^{-4}$ was formed immediately after vacuum transfer of CH_3I into vacuum adapted NMR tubes containing D_2O solutions of **6**. ^{1}H NMR (**6**) (D_2O, 360 MHz) δ (ppm): 8.81 (s, 8H, pyrrole), 8.39 (d, 4H, *o*-phenyl, $J_{1H-1H} = 7.2$ Hz), 8.30 (d, 4H, *o*-phenyl, $J_{1H-1H} = 7.2$ Hz), 8.23 (d, 4H, *m*-phenyl, $J_{1H-1H} = 7.2$ Hz), 8.19 (d, 4H, *m*-phenyl, $J_{1H-1H} = 7.2$ Hz), −6.59 (d, 3H).

Acid Dissociation Constant Measurements for $[(TSPP)Rh^{III}(D_2O)_2]^{-3}$ (2). Samples of $[(TSPP)Rh^{III}(OD)_2]^{-5}$ (**4**) were prepared by mixing a standardized solution of NaOH D_2O with the stock solutions of complex **1** ($(1.0-5.0) \times 10^{-3}$M) in NMR tubes. A series of HCl and NaOH deuterium oxide solutions were used to tune the pH values, and the $(TSPP)Rh^{III}$ pyrrole hydrogen ^{1}H NMR chemical shifts were recorded. A plot of the pyrrole hydrogen ^{1}H NMR chemical shifts to pD value (pD = pH + 0.45) is illustrated in Figure 1. Nonlinear least-squares curve fitting to the equation $\delta_{2,3,4(obs)}(pyr) = (K_1K_2\delta_4(pyr) + K_1[D^+]\delta_3(pyr) + [D^+]^2\delta_2(pyr))/(K_1K_2 + K_1[D^+] + [D^+]^2)$ gives K_1 =

$(1.4 \pm 0.2) \times 10^{-8}$, $K_2 = (2.8 \pm 0.3) \times 10^{-12}$, corresponding to eqs 1, 2. The equation is derived from the following analysis:

N_2, N_3, and N_4 are the mole fractions of rhodium complexes **2**, **3**, and **4**, respectively. δ_2(pyr), δ_3(pyr), and δ_4(pyr) are the chemical shifts for each of these species.

$$N_2 + N_3 + N_4 = 1, \quad K_1 = \frac{N_3}{N_2} \times [D^+], \quad K_2 = \frac{N_4}{N_3} \times [D^+]$$

$$N_3 = \frac{N_2 \times K_1}{[D^+]}, \quad N_4 = 1 - N_2 - N_3 = 1 - N_2 - \frac{N_2 \times K_1}{[D^+]}$$

Replace N_3 and N_4 with

$$N_3 = \frac{N_2 \times K_1}{[D^+]}$$

and

$$N_4 = 1 - N_2 - \frac{N_2 \times K_1}{[D^+]}$$

to the equation

$$K_2 = \frac{N_4}{N_3} \times [D^+]$$

then

$$K_2 = \frac{\left(1 - N_2 - \frac{N_2 \times K_1}{[D^+]} \times [D^+]^2\right)}{N_2 \times K_1}$$

So

$$N_2 = \frac{[D^+]^2}{K_1 \times K_2 + K_1 \times [D^+] + [D^+]^2}$$

is derived. Replace

$$N_2 = \frac{[D^+]^2}{K_1 \times K_2 + K_1 \times [D^+] + [D^+]^2}$$

with the equation

$$N_3 = \frac{N_2 \times K_1}{[D^+]}$$

and

$$N_4 = 1 - N_2 - \frac{N_2 \times K_1}{[D^+]}$$

$$N_3 = \frac{[D^+]^2}{K_1 \times K_2 + K_1 \times [D^+] + [D^+]^2} \times \frac{K_1}{[D^+]}$$

and

$$N_4 = 1 - \frac{[D^+]^2}{K_1 \times K_2 + K_1 \times [D^+] + [D^+]^2} - \frac{[D^+]^2}{K_1 \times K_2 + K_1 \times [D^+] + [D^+]^2} \times \frac{K_1}{[D^+]}$$

are obtained.

Replace the expressions N_2, N_3, and N_4 in the equation $\delta_{2,3,4obs}(pyr) = N_2 \times \delta_2(pyr) + N_3 \times \delta_3(pyr) + N_4 \times \delta_4$, and the equation

$$\delta_{2,3,4(obs)}(pyr) = \frac{K_1 \times K_2 \times \delta_4(pyr) + K_1 \times [D^+] \times \delta_3(pyr) + [D^+]^2 \times \delta_2(pyr)}{K_1 \times K_2 + K_1 \times [D^+] + [D^+]^2}$$

is derived.

Acid Dissociation Constant Measurement for [(TSPP)Rh−D]$^{-4}$ (5). HCl and [(TSPP)Rh^{I}]$^{-5}$ (**6**) (2.2×10^{-3} M) deuterium oxide solutions are degassed by three freeze−pump−thaw cycles and then carried into a glovebox. Samples with different pH values were obtained by mixing HCl and [(TSPP)Rh^{I}]$^{-5}$ (**6**) deuterium oxide stock solutions in NMR tubes. The total concentration of the rhodium species is within the range of $(1.2-1.8) \times 10^{-3}$ M. The tubes were taken out of the glovebox after being capped with a septum and sealed with Teflon tape. ^{1}H NMR spectra were recorded, and pH values were measured to determine the equilibrium distribution of rhodium(I) and rhodium hydride. A plot of the pyrrole hydrogen ^{1}H NMR chemical shifts to pD value (pD = pH + 0.45) is illustrated in Figure 3. Nonlinear least-squares curve fitting to the equation $\delta_{5,6(obs)}(pyr) = (K_5\delta_6(pyr) + [D^+]\delta_5(pyr))/(K_5 + [D^+])$ gives $K_5 = (8.0 \pm 0.5) \times 10^{-8}$, corresponding to eq 5. The curve fitting equation is derived from the following analysis:

N_5 and N_6 are the mole fractions of rhodium complexes **5** and **6**, respectively, and δ_5(pyr) and δ_6(pyr) are the pyrrole chemical shifts for each of these species.

$$N_5 + N_6 = 1, \quad K_5 = \frac{N_6 \times [D^+]}{N_5}$$

So

$$N_6 = \frac{K_5}{K_5 + [D^+]}$$

and

$$N_5 = 1 - N_6 = 1 - \frac{K_5}{K_5 + [D^+]}$$

Replace the expressions of

$$N_5 = 1 - \frac{K_5}{K_5 + [D^+]}$$

and

$$N_6 = \frac{K_5}{K_5 + [D^+]}$$

in the equation of $\delta_{5,6obs}(pyr) = N_5 \times \delta_5(pyr) + N_6 \times \delta_6(pyr)$, and then

$$\delta_{5,6(obs)}(pyr) = \frac{K_5}{K_5 + [D^+]}\delta_6(pyr) + \left(1 - \frac{K_5}{K_5 + [D^+]}\right)\delta_5(pyr)$$

$$\delta_{5,6(obs)}(pyr) = \frac{K_5 \times \delta_6(pyr) + [D^+] \times \delta_5(pyr)}{K_5 + [D^+]}$$

is obtained.

Analysis of $\Delta H°$ and $\Delta G°$(298 K) for Bond Homolysis of H−H, D−D, H−OH, and D−OD in Water. (a) The bond dissociation free energies (BDFE) and bond dissociation enthalpies (BDE) of the $(H-H)_g$ and $(H-OH)_g$ are derived from the formation free energies and

the formation enthalpies of H•, H_2, •OH, and H_2O, respectively ($\Delta_fG_g°$(H•) = 203.24 kJ mol^{-1}, $\Delta_fH_g°$(H•) = 217.94 kJ mol^{-1}, $\Delta_fG_g°(H_2)$ = 0 kJ mol^{-1}, $\Delta_fH_g°(H_2)$ = 0 kJ mol^{-1}, $\Delta_fG_g°$(•OH) = 37.4 kJ mol^{-1}, and $\Delta_fG_g°(H_2O)$ = −228.6 kJ mol^{-1} at 298 K),[23] ($BDFE_{(H-H)g}$ = 97.1 kcal mol^{-1}, $BDE_{(H-H)g}$ = 104.2 kcal mol^{-1}, $BDFE_{(H-OH)g}$ = 112 kcal mol^{-1}, and $BDE_{(H-OH)g}$ = 118.8 kcal mol^{-1} [24]). (b) The hydration energies of •H, •OH, and H_2O ($\Delta G_{hdy}°$(•H) = $\Delta G_{hdy}°(H_2) \sim +4.5$ kcal mol^{-1}, $\Delta G_{hdy}°$(•OH) ≈ −2.4 kcal mol^{-1}, $\Delta G_{hdy}°(H_2O) \approx -2.1$ kcal mol^{-1}, $\Delta H_{hdy}°$(•H) ≈ −1 kcal mol^{-1}, $\Delta H_{hdy}°$(•OH) ≈ −4.8 kcal mol^{-1}, and $\Delta H_{hdy}°(H_2O) \approx -10.5$ kcal mol^{-1})[25] are used in combination with the BDFE and BDE of $(H-H)_g$ and $(H-OH)_g$ to evaluate $BDFE_{(H-H)aq}$ = 101.8 kcal mol^{-1}, $BDE_{(H-H)aq}$ = 103.2 kcal mol^{-1}, $BDFE_{(H-OH)aq}$ = 116.1 kcal mol^{-1}, and $BDE_{(H-OH)aq}$ = 123.5 kcal mol^{-1}. (c) The BDFE and BDE of $(D-D)_{aq}$ and $(D\text{-}OD)_{aq}$ are estimated on the basis of the corresponding H−H and H−OH values and the zero-point energy difference of (H−H) with (D−D) (∼1.7 kcal mol^{-1}) and (H−OH) with (D−OD) (∼1.5 kcal mol^{-1}) resulting from the streching frequency difference ($BDFE_{(D-D)aq}$ = 103.4 kcal mol^{-1}, $BDE_{(D-D)aq}$ = 104.5 kcal mol^{-1}, $BDFE_{(D-OD)aq}$ = 117.6 kcal mol^{-1}, and $BDE_{(D-OD)aq}$ = 124.8 kcal mol^{-1}).

Acknowledgment. The authors acknowledge support of this research from the Department of Energy, Division of Chemical Sciences, Office of Science through grant DE-FG02-86ER-13615.

JA039218M